UNIVERSIDADE da MADEIRA

A Nossa Universidade

www.uma.pt

FCEE

Mestrado em Engenharia Informática

Exploiting IoT-enabled Inertial Sensors for Position Estimation

Cláudio Rodrigues

supervisionado por

Marko Radeta and Filipe Quintal

24 de setembro de 2021

Abstract

With the surge of inexpensive, widely accessible, and precise microelectromechanical systems (MEMS) in recent years, inertial systems tracking movement have become ubiquitous nowadays. Contrary to GPS-based positioning, Inertial Navigation Systems (INS) are intrinsically unaffected by signal jamming, blockage susceptibilities, and spoofing. Measurements from inertial sensors are also acquired at elevated sampling rates and may be numerically integrated to estimate position and orientation knowledge. These measurements are precise on a small-time scale but gradually accumulate errors over extended periods. Combining multiple inertial sensors in a method known as sensor fusion makes it possible to produce a more consistent and dependable understanding of the system, decreasing accumulative errors. Several sensor fusion algorithms occur in literature aimed at estimating the Attitude and Heading Reference System (AHRS) of a rigid body with respect to a reference frame. This work describes the development and implementation of a low-cost, multipurpose INS for position and orientation estimation. It presents an experimental comparison of the most popular sensor fusion solutions. Additionally, the study explores the prospect of integrating transmission Internet of Things (IoT) devices (based on an open radio frequency at 868 MHz) to broadcast in real-time and at a long distance the navigational data of a moving object and how this approach may be employed in a series of real-world scenarios.

Keywords: Sensor Fusion · Inertial Navigation System (INS) · Microelectromechanical system (MEMS) · Internet of Things (IoT) · Inertial Measurement Unit (IMU) · Aerial Assessments

Resumo

Keywords: Ubiquitous Computing · Aerial Assessments · Wildlife Monitoring · Machine Learning · Application Development · Low-Altitude Balloons.

Acknowledgements

Cláudio Rodrigues

Table of Contents

List of Figures

List of Tables

1 Introduction

Navigation systems have become a popular subject in the designing of unmanned and autonomous systems in recent years. Still, most navigation systems highly depend on the Global Navigation Satellite System (GNSS) receivers as the central resource of navigation data. Although the satellite system can deliver accurate and long-term positioning in open spaces, when relying on GNSS only localization, there are often circumstances when the satellite signal is obstructed or weakened, resulting in degradation or even loss of position estimate precision [14]. Such is especially threatening in high urbanized centers where satellite signals can suffer multipath propagation from tall glass-covered buildings [32]. Satellite positioning is especially impactful in battery autonomy, whereas GNSS receivers remain draining a substantial amount of electric current. Inevitably, there is a need to become less dependent on GNSS-based localization, particularly in autonomous settings. Substantial research has been conducted to enhance the localization precision of an object devoid of satellite signals [29] [6] [17] [5] [43]. Increased accuracy is a precursor to establishing autonomous agents for a diversity of functions. Inertial measurement units (IMU) have become standard in embedded inertial systems due to their low cost, lightweight, and low power consumption. They can provide short-term position and orientation changes. Furthermore, inertial systems have been employed in wearable applications with uses in unmanned aerial vehicles (UAV) [12] [24] [36], telemedicine [26], and robotics [42]. Despite these accomplishments, inertial systems suffer from rapid drift owing to the existence of disturbances and noise in the measurements. Practically all present commercial applications are restricted to minimal motion recognition. Position and orientation in real-world applications are rarely employed due to difficulties in precise integration. Recently, innovative fusion algorithms have emerged, which can diminish the impacts of noise and disturbances, broadening these devices' capabilities. There is an increasing need, which remains unmet, for inertial orientation and position applications since they are key to automation and the "Internet of Things" (IoT). We propose a low-cost, multipurpose inertial solution exploring the Internet of Things with modules for an Inertial Measurement Unit that may support maintaining high levels of orientation and location exactness even when satellite-based location is not possible.

1.1 Problem Statement

This dissertation explores three core challenges that remain with significant interest in literature.

1.1.0.1 A. GNSS only positioning is prone to signal jamming and impacts battery autonomy

Modern navigation relies greatly on the Global Navigation Satellite System (GNSS) constellations (such as GPS, Galileo, GLONASS, etc.); being straightforward to operate, accurate and trustworthy, it is widely employed in navigation systems. Nevertheless, GNSS signals still encounter numerous vulnerabilities and can often be compromised by natural and human sources [14]. Attacks against GNSS-based localization are becoming more frequent and of intensifying damage [33]. Satellite signals can also be affected by abnormal activity due to solar winds, creating temporary gaps in coverage [1]. Moreover, while GNSS offers seamless navigation with inexpensive receivers, they are also prone to signal jamming, where satellites are unable to detect the objects. Repeatedly, position accuracy is reduced or even lost, such as in tunnels or underground sections [34] [32]. Furthermore, GNSS cannot accurately determine altitude with the necessary exactness, which is essential to accurately depict a body in three-dimensional space. Lastly, localization technologies demand high processing capacity and communication costs. This is particularly impactful in autonomous settings, where battery autonomy is crucial, while GNSS receivers continue to drain a large amount of electric current [21]. Consequently, power optimization is critical, and there is a necessity to become less reliant on GNSS-based localization.

1.1.0.2 B. Dead reckoning is susceptible to cumulative errors and suffers from gimbal lock

When understanding the alternatives to GNSS for estimating the position, the dead reckoning technique is often employed to resolve the location of a moving object. Using sensor data (gyroscope, accelerometer, magnetometer, etc.), it is possible to assess current position even when GNSS positioning is not possible [32]. It has been recognized as a low-power alternative to GNSS localization that can deliver high-resolution position data [6]. It is possible to estimate the current position from an obtained distance (which may be estimated from velocity), the known starting point, and estimated drift. However, the precision of the dead-reckoning approach is continuously worsening while measurement errors accumulate during the current position estimation [17]. The approach is also embedded in Kalman filtering and other fusion techniques (will be explored in Section II), which mathematically merges a series of navigation solutions to obtain the best estimate of the navigator's current position, velocity, attitude angles, etc [19].

Still, precise tracking of a moving and rotating body in three-dimensional space implies a superior degree of complexity (compared to two-dimensional tracking). It can be accomplished in a range of approaches. Most commonly, the orientation of bodies that move in three dimensions may be explained by a combination of their angle of rotation across each of their three axes (e.g., such as in trigonometry, where Euler angles can approximate yaw, roll, and pitch). Fundamentally, a specific movement could be defined by multiple rotations. In such case, to perform a rotation over a particular axis, rotational matrices, vector operations, and trigonometric functions are required [3]. This involves numerous complex mathematical operations and several clock cycles in a microprocessor that could negatively impact computational performance [16].

Nevertheless, the rotation axes are not always independent, and results are not necessarily distinctive or unique. This further implies that the plane of two gimbals (rotational axes) to align, which causes the recognized gimbal lock phenomenon, where two out of three gimbals are parallel or very nearly parallel (such as in figure 1.b), reducing the output to two degrees of freedom [11]. When gimbal lock happens, it is not possible to reorientate the axes without an external reference.

1.1.0.3 C. Gravity acceleration greatly impacts sensor readings

An accelerometer is generally utilized to estimate the velocity and position of a given body devoid of the usage of GNSS. These electromechanical devices can measure proper acceleration forces, which can be employed to determine a body's velocity and position relative to a starting point. In theory, this can be done by integrating the resultant of acceleration yielding velocity; double integrating will deliver the body's accumulative position [44]. In practice, these measurements are influenced by Earth's gravitational field and rotational components of acceleration, significantly magnifying numerical errors during the readings [30]. The gravity component will not be differentiated from the physical acceleration of the device and will eventually generate exceedingly elevated errors in the measured acceleration. Double integrating these

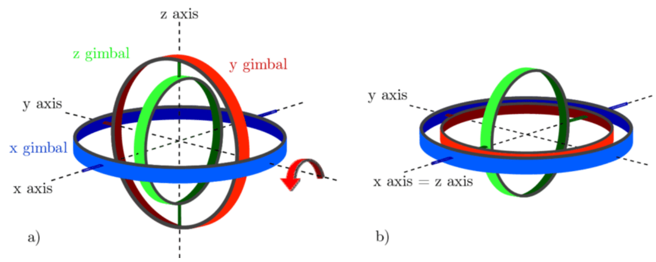

Fig. 1: Representation of the Gimbal Lock problematic [45] - The exterior blue gimbal characterizes the x-axis, the middle, red-colored gimbal the y axis, and the inner green gimbal the z-axis. In the initial arrangement a), every axis is perpendicular to one another. Following a rotation of 90º across the red arrow (y-axis), the blue and the green gimbals occupy the same rotation axis. This condition inhibits the clear determination of the rotation axes when subsequently rotating around the x or z-axis.

measurements will inherently amplify errors which will accumulate exponentially, translating into a yet greater offset in velocity and position estimates [39].

A potential solution to minimize this difficulty is to assume the body moves on a flat surface, thus greatly diminishing the influence of the gravity component on acceleration readings. Every inaccuracy that may arise from hiring such supposition can be regarded as noise and is smoothly filtered [30]. Understandably, such an assumption is not possible with a body moving through three-dimensional space since it is subject to many kinds of forces and movements. A numerical process is required for handling accelerometer measurements that utterly removes the effect of the gravity component and further undesirable acceleration vectors.

1.2 Research Questions

While research has been performed towards orientation estimation by the fusion of multiple sensors, few studies sought to assess position due to difficulties removing the measurement of normal forces that do not cause physical acceleration of the sensor. This investigation seeks to comprehend how different sensor fusion approaches perform in approximating the orientation of a moving system, along with how to overcome the positioning challenge through a technique that combines orientation estimation to filter non-physical acceleration. Additionally, we examine how the Internet of Things can be applied to perform telemetry in real-time and at a long distance of a moving object.

– **[RQ1]. Estimate** - How to perform a low-cost orientation and position estimation of a moving object devoid of GNSS?
  The study will emphasize on the possibility of estimating the orientation and position of a moving object in three-dimensional space short of GNSS-based positioning by combining multiple low-cost sensors to provide an object's navigation information.

– **[RQ2]. Comparing** - How distinct fusion techniques perform in orientation and position estimation?
  An experimental comparison between various sensor fusion algorithms is used to evaluate how accurate each approach can approximate orientation and position.

– **[RQ3]. Communicate** - How to transmit navigational data in real-time at a long-distance?
  Lastly, this dissertation will explore the prospect of amalgamating transmission IoT devices (based on open radio frequency at 868 MHz) to broadcast in real-time and at a long distance the navigational data of a moving object and how this approach may be employed in a series of real-world scenarios.

2 Related Work

The literature review is divided into subsequent sections: 1) Position estimation using inertial sensors systems. 2) Sensor fusion in position and orientation estimation.

2.1 Position estimation using inertial sensor systems

Inertial sensor systems have been thoroughly researched with the purpose of delivering position estimation of a moving body. Inertial systems are autonomous and independent and do not rely on external information, such as radio signals or electromagnetic waves. Their navigation data have short-term high accuracy, great constancy, and elevated data update rate. They may be applied in an array of distinct positioning methods.

2.1.1 Pedestrian Dead Reckoning

Pedestrian dead reckoning (PDR) is among the most explored. PDR combines step detection, step length estimation, and orientation approximations to calculate the absolute position and heading of a walking user. PDR can operate with a single accelerometer, although superior precision and robustness are obtained with more sensors. An Inertial Measurement Unit (IMU) containing several accelerometers, gyroscopes, magnetometers, and even pressure sensors are commonly employed to recognize steps and orientation. Sensors might be body-mounted or shoe-mounted. Pedestrian navigation systems can aid the blind and visually impaired, locating and rescuing firefighters and other emergency workers, hiking, sports, and others. Pedestrian dead reckoning is commonly reviewed in the literature, being subject to studies in various settings.

Ladetto et al. [20] applied PDR in urban and indoor areas seeking to assist blind people reaching unfamiliar locations along with aiming to facilitate emergency coordinators to track rescue workers. The study integrated a GPS receiver with a body-mounted IMU applying pattern recognition to accelerometer signals, determining a user's step signature.

Stirling et al. [38] illustrate an experiment exploiting a shoe-mounted sensor prototype that calculates stride length with accelerometers and magnetometers. Their system measures angular acceleration by manipulating pairs of accelerometers as an alternative to gyroscopes.

Several other studies investigate the prospect of using inertial sensor systems to estimate the absolute position and heading of a walking user for multiple purposes [37] [40] [18] [4]. The main drawback of PDR is its dependence on step prediction algorithms that must distinguish step direction and step lengths as the user changes pace.

2.1.2 Strapdown Inertial Integration

Strapdown inertial integration or strapdown inertial navigation system (SNIS) is another prevalent position method. With SNIS, sensors are usually tightly strapped or attached to the axes of the moving body's structure, lowering costs and enhancing the system's reliability. This technique integrates accelerometer and gyroscope measurements to distinguish the variation of position and heading. The strapdown system demands a high-level measurement rate, on average, beyond 2000 Hz. Typically, higher measurement rates translate into more accurate integration readings of position and attitude. Strapdown systems are currently employed in commercial and military applications (airplanes, vessels, ROVs, projectiles) and are a topic of study among scholars.

Jameian et al. [15] introduced strapdown inertial navigation system to nautical environments, proposing a compensation method against disturbing forces affecting vessel motion caused by rough sea conditions. They aim to resolve attitude determination offset through self-alignment of SNIS by establishing vector observations. The implementation makes use of a quaternion estimator for attitude determination, significantly diminishing computational complexity.

An indoor strapdown inertial navigation with small foot-mounted and self-contained sensor systems was described by Bird et al. [2]. Similar to pedestrian dead reckoning, SNIS also has applications in pedestrian navigation systems, although operating in an utterly distinct fashion. Unlike PDR, the strapdown navigation algorithm traces the entire movement of the foot in between steps. Any movement like walking, running, climbing up or down, moving backward or sideways, sliding, and even jumping can be tracked. This is possible because of a zero-velocity update algorithm (ZVU) which exploits the brief periods of zero velocity when the feet are stationary on the ground.

SNIS and PDR may also be used together, sharing the same inertial sensors. In this case, inertial navigation is incorporated within the multi-sensor integration architecture as the reference system and PDR as an aiding sensor.

With a focus on low-cost inertial motion sensors, Coyte et al. [5] applied PDR to sporting training and rehabilitation. They propose solutions to acceleration noise accumulation and gyroscope angle error problems. To improve the accuracy of displacement estimation with a low-grade IMU, they developed a zero-velocity update algorithm.

2.2 Sensor fusion in position and orientation estimation

Sensor fusion defines the blending of sensory information from two or more sources in a way that generates a more consistent and dependable understanding of the system. One that would otherwise not be possible when these sources were used individually [10]. Fusing multiple inertial systems has raised significant interest and consideration in location and attitude performance improvement. Numerous methods arose in recent times that merge information from various systems such as inertial sensors, GNSS, radar, radio telescopes, signal of opportunity systems like Angle of Arrival (AOA), Time of Arrival (TOA), Received Signal Strength (RSS), and Signal to Noise Ratio (SNR). The combination of multiple sources can help reduce noise with two different sensor types. These separate systems are integrated by fusion filter algorithms which process each input and generate a more precise and reliable output [8]. A substantial sum of distinct solutions designed to assess the orientation of a rigid body regarding a reference frame exist in literature. Two main approaches aimed at sensor fusion exist, Kalman and complementary related filters. A comprehensive analysis of the literature will be conducted seeking to better understand the distinction between algorithms and how do they compare.

2.2.1 Kalman filter

The Kalman filter algorithm is a set of mathematical equations that provides a computationally efficient approach to estimate some unknown variables by the detected measurements [41]. Kalman filters operate recursive functions to predict the present state of a linear problem by monitoring the current input data, the previous input data, and the previous state prediction. Two generally assigned methods for Kalman filter-based sensor fusion are state-vector fusion and measurement fusion. The state-vector fusion method (figure 2a) applies a group of Kalman filters to acquire individual sensor-based state estimates, which are subsequently fused to obtain an enhanced combined state estimate. Measurement fusion (figure 2b) approach directly combines the sensor data to achieve a joint measurement and later uses a single Kalman filter to get hold of the final state estimate centered on the fused measurement [28]. When applied appropriately, Kalman filters offer highly precise orientation, even with the existence of substantial noise. Nevertheless, Kalman filters are computationally expensive rising hardware cost and latency. They are also of complex implementation, which, shared with computational overhead, can make the algorithm unfeasible for computationally restricted applications. They are regularly useful in a wide-ranging variety of applications and have become a standard method in sensor fusion. Several studies examine the possibility of using Kalman filters to predict a body's orientation and position by combining multiple sensors. The Kalman filter is founded on recursive Bayesian filtering.

Consequently, the system's noise is assumed to be Gaussian. Therefore, the Kalman filter is generally suggested for linear systems. For this reason, an extension of the classic Kalman Filter designed for non-linear systems has emerged, recognized as Extended Kalman filter [42].

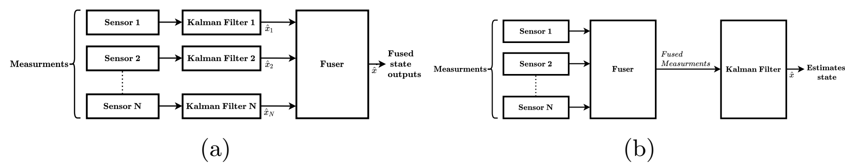

Fig. 2: Kalman-filter-based multi-sensor data fusion. (a) State-vector fusion. (b) Measurement fusion. [28]

Several research works have been conducted on Inertial Navigation Systems and Global Navigation Satellite System integration through data fusion, particularly using the Kalman filter. To overcome the shortcomings linked to the detached functioning of GNSS and INS, Wong et al. [43] Qi et al. [35], and Nassar et al. [29] combined both systems so that their disadvantages were lessened or eradicated, complementing one another. While GNSS was comparatively more stable and consistent for long periods, INS had a more reliable and comprehensive short-term signal. Updating INS position and velocity with GNSS data corrected error expansion at the same time it delivered more precise estimates. The Kalman Filter attempted to adjust INS information based on the system error model whenever GNSS signals were interrupted or limited. These studies have demonstrated success in satisfying the accuracy requirements of low-precision applications. However, they could not deliver the high-precision positioning some applications required. Hence, other studies attempted to achieve better performance of integrated INS/GNSS systems through the exploration of extended and adaptive Kalman filtering techniques. Mohamed and Schwarz [27] performed an analysis on INS/GNSS alternative integration through an adaptive Kalman filtering technique. Findings reveal that their adaptive Kalman filter outperformed by almost 50% the conventional filter.

The use of data fusion in autonomous flying units such as Unmanned Aerial Vehicles (UAV) has recently gained particular concern due to the dissemination of consumer-grade quadcopters. In autonomous aerial settings, an accurate altitude reading is crucial to control the position of the flying system. However, such measurements are repeatedly corrupted with signal noise produced by the vehicle's motors. Hetényi et al. [12] applied a Kalman Filter to fuse the sonar and accelerometer signals, obtaining a considerably improved altitude estimate with minimal error. Similarly, Luo et al. [24] combined the UAV sensor system and received signal strength (RSS) in a Kalman filter solution. The study sought to increase position and altitude estimation as well as collision avoidance precision by approximating the distance between the receiver and the transmitter via the use of radiofrequency signals reducing the noise component.

Sharma et al. [36] present an experiment of Kalman filter-based sensor fusion for extrapolation of a robot's orientation and depth to obstacle by fusing the inputs from three infrared sensors and an inertial sensor system. The combination of multiple sensor inputs allowed the robot to operate in fault-tolerant applications and enhanced its obstacle avoidance decision making, localization, and orientation estimations.

2.2.2 Complementary filter

The complementary filter is considered a simpler approach relatively to the Kalman filter since it is a computationally lightweight solution and straightforward to implement [13]. This filter takes as input two noisy sensor measurements and assumes one input is mainly formed by high-frequency signals whereas the other is mostly by low-frequency signals. Through a low pass filter, the high-frequency noise of the first input is filtered out. An identical procedure occurs with the second signal, but this time with a high pass filter to remove low-frequency noises, as illustrated in figure 3. Yet, the complementary filter is not especially robust to noisy or biased data since it simply uses currently available information, therefore, has no direct method of compensating for sensor noise [42]. A conventional application of the complementary filter is to bring together measurements of vertical acceleration and barometric readings to attain an approximation of vertical velocity. Similar to the Kalman filter, new versions built upon the principles of the classic complementary filter have emerged in recent times, such as the Extended Complementary Filter (ECF). They promise a high level of accuracy and enhanced robustness to noise while preserving computational efficiency.

Madgwick et al. [26] outlined the formulation of an extended complementary filter algorithm and exhibited its applicability as a human motion monitoring

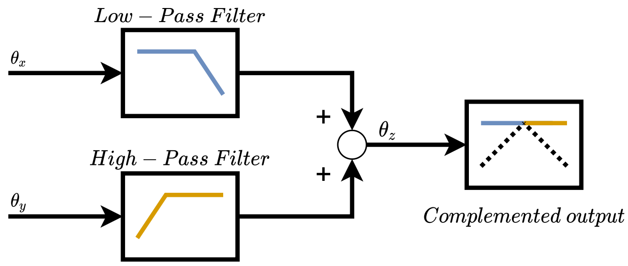

Fig. 3: Basic complementary filter [13] - Two different measurement sources for estimating one variable. The noise properties of the two measurements are such that one source gives good information only in low frequency region while the other is good only in high frequency region.

wearable. Their design fused magnetic, angular rate, and gravity sensor data to remotely estimate limb orientation in stroke patients performing rehabilitation exercises. They analyzed performance under a range of circumstances and benchmarked alongside other frequently utilized sensor fusion algorithms. They claim an improved computational efficiency of over 30% when compared with standard alternative algorithms.

A complementary filter designed for sensor fusion in quadrotor UAV employing a low-cost inertial measurement system was proposed by Noordin et al. [31]. The complementary filter filtered high-frequency signals associated with the gyroscope and low-frequency signals linked to the accelerometer. Findings demonstrate that the complementary filter technique overcame the over drift conundrum related to gyroscopes and was capable of computing attitude angles efficiently. Euston et al. [9] conducted an analogous study with a non-linear complementary filter for attitude estimation in a UAV utilizing a low-cost IMU. They broadened the experiment to incorporate a model of the longitudinal angle-of-attack corresponding to the UAV's airframe acceleration using airspeed data. As a result, they could estimate the acceleration of the UAV during continuous turns based on gyroscope and airspeed data. They accomplished attitude filtering performance of similar quality as an extended Kalman filter that fused GPS/INS at a far less computational cost.

2.2.3 Optimization filters

Up until recently, there remained mainly two distinct AHRS fusion approaches. One category including the complementary filters, and the other is related to

Kalman filtering. Some recent AHRS algorithms have emerged in the literature over the past years. Two of the most prominent are the Mahony and Madgwick algorithms, which have been categorized as optimization filters. Optimization filters obtain orientation by assessing a vector representative of the sensor output at the present orientation and lessening the disparity concerning predicted and observed outputs. Optimization filters are well established for linking accuracy with computational expense and simplicity of implementation [26]. Both methods make use of a quaternion representation, which is a four-dimensional complex number representing of an object orientation. Quaternions involve fewer computation time because of their minimal quantity of calculation parameters [22]. Additionally, vector rotations are easily executed by quaternion multiplications. Madgwick et al. [25] pioneered a gradient descent fusion algorithm, frequently recognized as 'Madgwick Algorithm.' This gradient descent fusion algorithm first obtains a quaternion estimation of the gyroscope output integration and later corrects it with a quaternion from the accelerometer and magnetometer data. Madgwick's approach guarantees decent attitude estimation at a low computational cost. Further, it tackles the difficulty of the local magnetic disturbances that can influence all the orientation components. By reducing the constraint of the magnetic field vector rotation, it can limit the effect of the magnetic disturbances to only affect the yaw component of the orientation.

2.2.4 Sensor fusion algorithms comparison

Some studies have conducted comparison experiments between the sensor fusion algorithms in distinct settings to assess their performance in that unique condition. Ludwig et al. [22] compared Madgwick and Mahony in a foot-mounted experiment. Their findings revealed that Madgwick achieved better heading orientation than Mahony when compared to the ground truth. Nonetheless, the performance of Mahony was superior to Madgwick. The same authors tested on [23] quadcopters the Extended Kalman Filter, Madgwick, and Mahony filters. Results showed that Mahony delivered a more precise orientation estimation and faster execution time than Madgwick and EKF. Diaz et al. [7] present a comparison among Madgwick and Mahony, a basic AHRS estimation algorithm, and the recent algorithm proposed by the authors. The study centered around comparing the performance of Madgwick, Mahony, Extended Kalman Filter, and their own sensor fusion algorithm, emphasizing the behavior under magnetic perturbations. Various examples of movement were analyzed, from carrying the sensor at separate places such as pocket, shoe, and hand. They concluded that their algorithm was slightly less influenced by magnetic perturbations than the others, but overall, the algorithms performed similarly.

2.3 Thesis Contribution

With this study, we aim to design and build a low-cost, multipurpose Inertial Navigation System, intending to estimate the orientation and position of a moving object in three-dimensional space. This research additionally proposes introducing an experimental comparison among several established AHRS sensor fusion algorithms such as the Extended Kalman Filter, Madgwick, and Mahony algorithms. Furthermore, a quaternion-based gravity compensation filter will be presented, diminishing the influence of the gravity component on acceleration readings. Our key contribution is to merge IoT with our Inertial System through Long Range (LoRa) communication to perform real-time and long-distance telemetry.

3 Methodology

This section provides a hardware and software solution outline, describing the development and implementation of a low-cost, multipurpose Inertial Navigation System with experimental tests. Resultant findings are analyzed and validated to assess the implemented system's positioning and orientation (AHRS) effectiveness and precision. Several fusion algorithms will be benchmarked by performance and accuracy. This development was achieved mainly in three phases, system design, hardware application, and software implementation.

3.1 Evaluation Methodology

3.1.1 Obtaining AHRS from sensor fusion

The first experiment involved obtaining orientation (AHRS) from the fusion of the three sensor outputs. The accelerometer provided the system's proper acceleration; the gyroscope supplied the body's angular rate, and the magnetometer presented the detected magnetic flux. In this first experiment, we first utilized the Madgwick algorithm to sensor fusion for its well-recognized proficiency to merge accuracy with computational cost and simplicity of implementation. A simple test was performed using a box containing the inertial navigation system and rotating around its three inertial axes, pitch, roll, and yaw, with a sampling frequency of 20 Hz. The raw output measurements from the sensors are visualized in figure 9 and are subsequently taken as input by the sensor fusion algorithm.

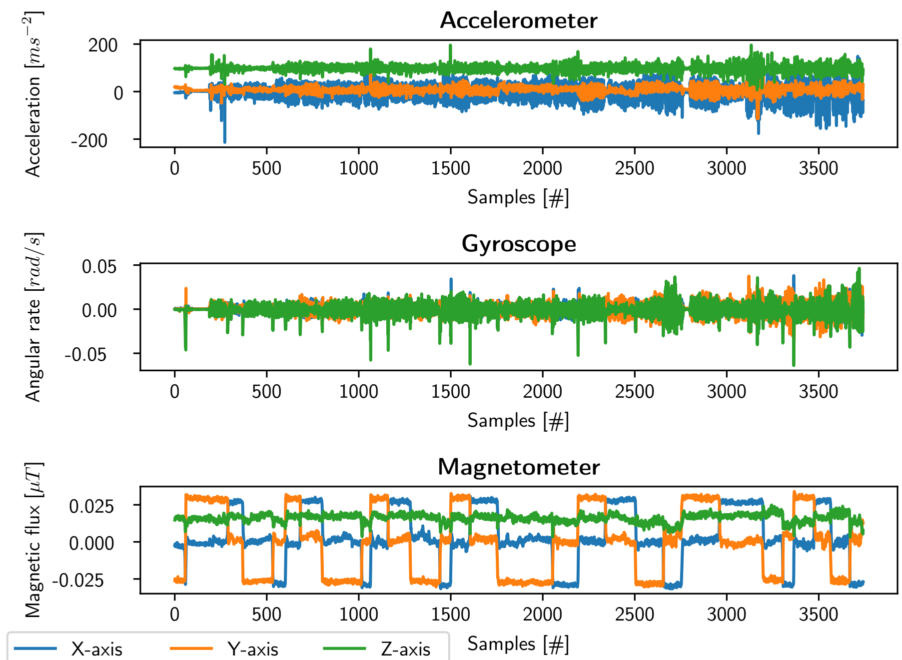

Fig. 4: Sensor data on each axis (blue is X-axis, red is Y-axis, green is Z-axis) obtained by the accelerometer, gyroscope, and magnetometer at 100 Hz sampling rate. Accelerometer provided the system's proper acceleration; gyroscope supplied the body's angular rate, and the magnetometer presented the detected magnetic flux.

The fusion output is shown in figure **??**. About sample #140 there was a shift in pitch to -40º and later jumping to 40º. Around sample #350 there is a change in roll to 60º and then -40º, and around sample #540 there is a variation in yaw value. This output is analogous to the movement made on the board.

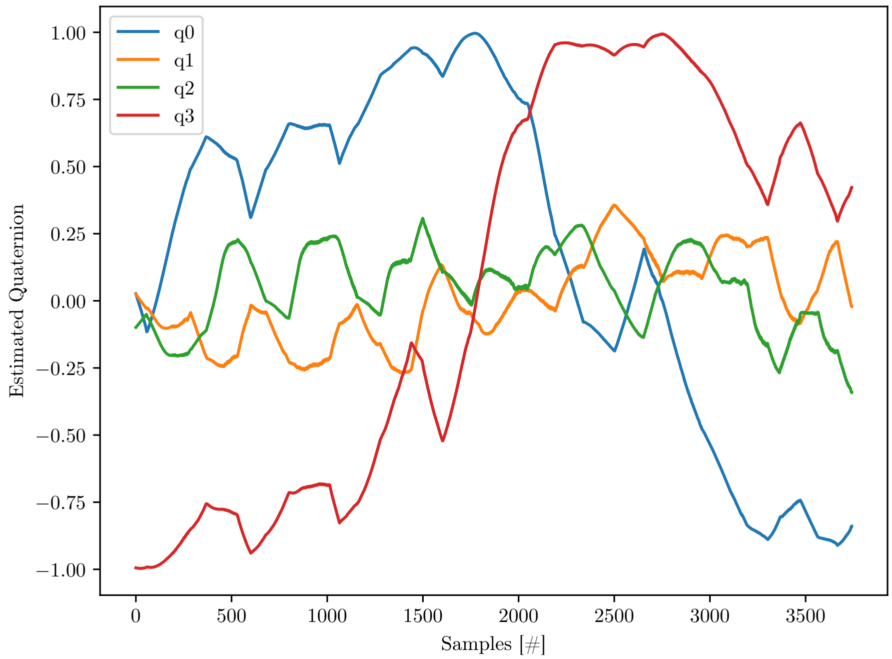

Fig. 5: Sensor data on each axis (blue is X-axis, red is Y-axis, green is Z-axis) obtained by the accelerometer, gyroscope, and magnetometer at 100 Hz sampling rate. Accelerometer provided the system's proper acceleration; gyroscope supplied the body's angular rate, and the magnetometer presented the detected magnetic flux.

3.1.2 Estimating position

Accelerometer readings can measure proper acceleration forces, which can be employed to determine a body's velocity and position relative to a starting point. Integrating the resultant of acceleration will yield velocity, and double integrating will provide the body's accumulative position.

Once the measured inertial-frame acceleration is attained, it can be integrated to obtain inertial frame velocity v_i and position x_i can be calculated:

$$v_i = v_0 + \int^t a_i \, dt \tag{1}$$

$$x_i = x_0 + \iint^t a_i \, dt \tag{2}$$

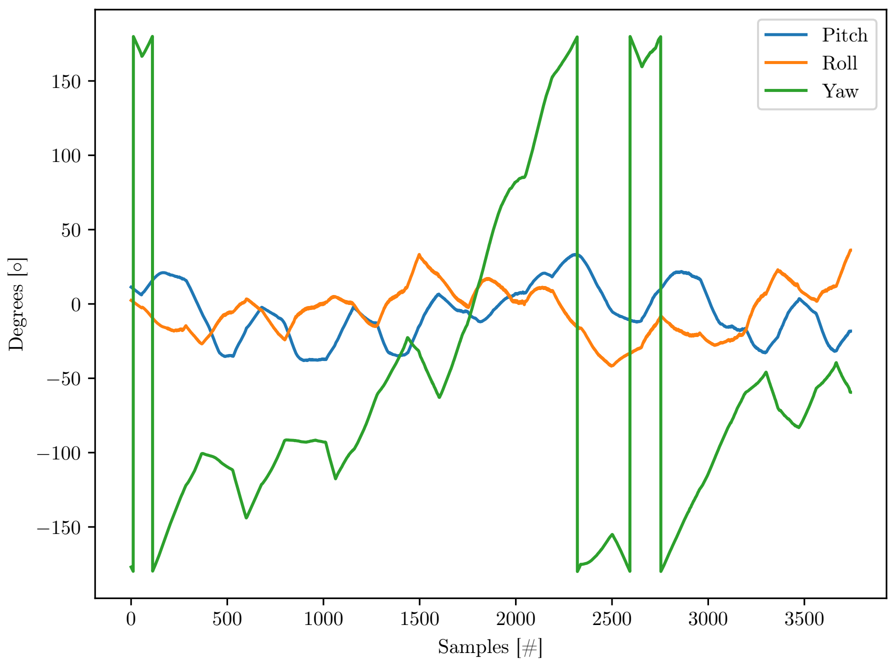

Fig. 6: Sensor data on each axis (blue is X-axis, red is Y-axis, green is Z-axis) obtained by the accelerometer, gyroscope, and magnetometer at 100 Hz sampling rate. Accelerometer provided the system's proper acceleration; gyroscope supplied the body's angular rate, and the magnetometer presented the detected magnetic flux.

In practice, data is acquired at discrete time periods (Δt) so the approximate velocity and position are estimated by:

$$v_i[k+1] = v_i[k] + a_i[k]\Delta t \tag{3}$$

$$x_i[k+1] = x_i[k] + v_i[k]\Delta t \tag{4}$$

However, these measurements are affected by the Earth's gravitational field (as seen in figure 9 in the acceleration readings) and rotational components of acceleration, considerably amplifying numerical errors. The gravity component will not be differentiated from the physical acceleration of the device and will eventually generate exceedingly elevated errors in the measured acceleration. To overcome this challenge, a gravity compensation algorithm is crucial for subtracting the impact of the gravity component on acceleration readings. Through orientation estimation determined previously, it is possible to find the orientation of the Earth frame with respect to the sensor frame. Therefore, compute the expected direction of gravity and then subtract that from the accelerometer readings (figure **??**). Resulting in a linear acceleration that corresponds to the physical acceleration of the device. This linear acceleration can be numerically integrated returning velocity and double integrating delivering the position of the device (figure 8).

The next step consisted of experimentally testing the inertial system seeking to achieve position estimation merely by integrating the accelerometer measurements with the gravity compensation filter. Numerous experiments were performed in several settings. The tests involved walking on a straight line carrying a box containing the inertial system (with the inertial X-axis parallel to the path) for around 30 meters, evaluating the computed acceleration, velocity, and accumulative position estimation. Specific tests were executed at walking pace, others at running pace, and some with a combination of both.

First, one-dimensional experiments were conducted, pursuing to estimate accumulative position when moving on a straight line for 30 meters. These tests revealed an average error margin from 10% to 15% of the actual distance. Different movements and walking paces were tested, such as stopping at different time intervals. With the accomplishment of this first experiment, we

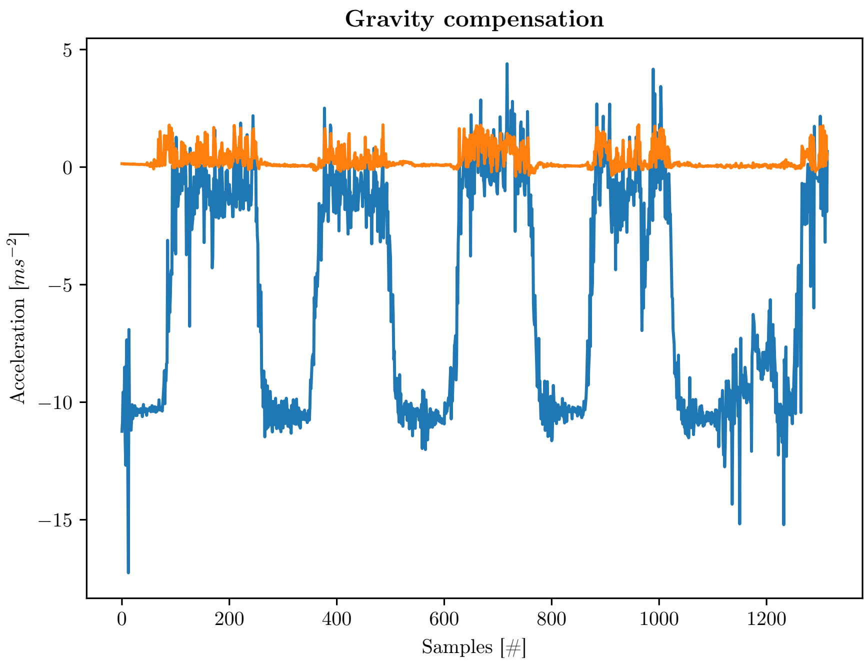

Fig. 7: Sensor data on each axis (blue is X-axis, red is Y-axis, green is Z-axis) obtained by the accelerometer, gyroscope, and magnetometer at 100 Hz sampling rate. Accelerometer provided the system's proper acceleration; gyroscope supplied the body's angular rate, and the magnetometer presented the detected magnetic flux.

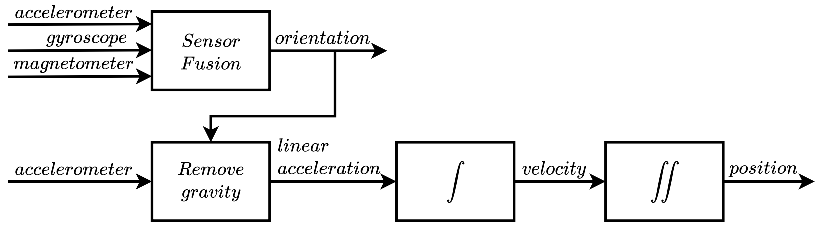

Fig. 8: Overview of the position estimation method.

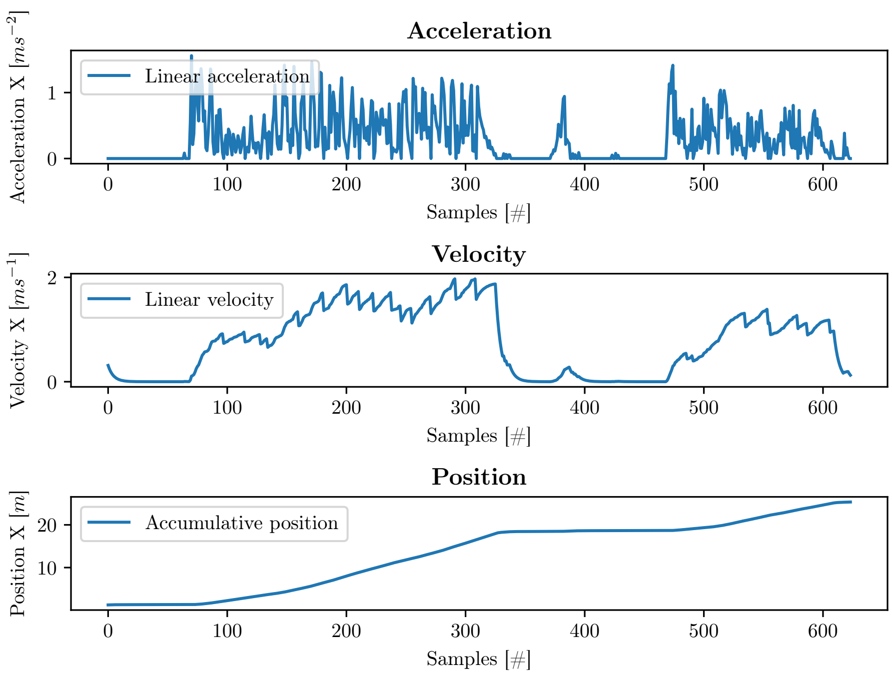

Fig. 9: Sensor data on each axis (blue is X-axis, red is Y-axis, green is Z-axis) obtained by the accelerometer, gyroscope, and magnetometer at 100 Hz sampling rate. Accelerometer provided the system's proper acceleration; gyroscope supplied the body's angular rate, and the magnetometer presented the detected magnetic flux.

decided to expand the testing to two dimensions. An experiment result is observed in figure **??**, where the final observed accumulative position was 25 meters.

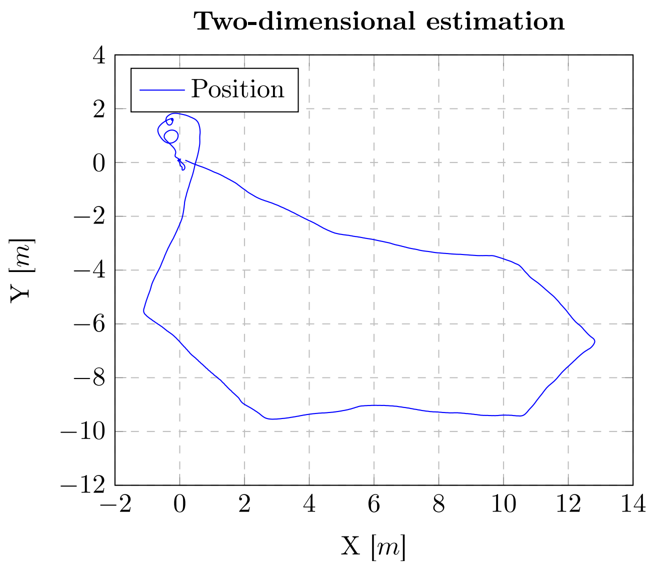

Fig. 10: Experiment combined X-axis and Y-axis accelerometer measurement with orientation estimation. Conducted test involved walking counterclockwise on a circular shape of around 8 meters in diameter.

In two-dimensional tests, the output from X-axis and Y-axis accelerometer measurements were integrated with orientation to acquire accumulative position on both axes. These tests implicated moving on a linear pattern, generally 10 meters on each axis. Integrated axis position was then plotted into a scatter plot that combines the accumulative position on the two axes. Figure 10 shows an experiment performed with two-dimensional positioning.

Finally, only the three-dimensional experiment was left combining the output readings from the Z-axis accelerometer. The same previous procedure was employed in this experimentation; the output from X-axis, Y-axis, and Z-axis accelerometer measurements were combined with orientation and integrated to obtain an accumulative position on all axes. A similar movement to the two-dimensional test was performed, but this time wobbling the inertial unit vertically to better visualize the position variation on the Z-axis. An example of an experimental test conducted in three dimensions in visible is figure 17.

Fig. 11: 5 meter side ground square used for baseline of accuracy of inertial system.

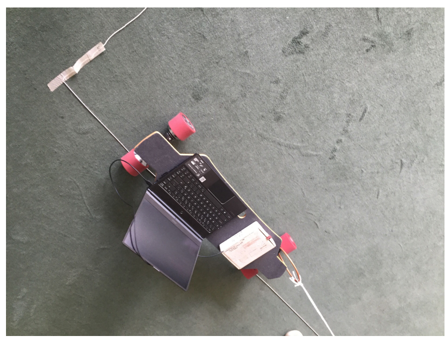

Fig. 12: Experiment made with skateboard to assess localization accuracy.

Fig. 13: Manually pulling the skateboard on each side of the ground square.

3.2 System Architecture

As our projected solution involved a low-cost navigation system, the hardware selection criteria were primarily founded on availability and cost. The cost

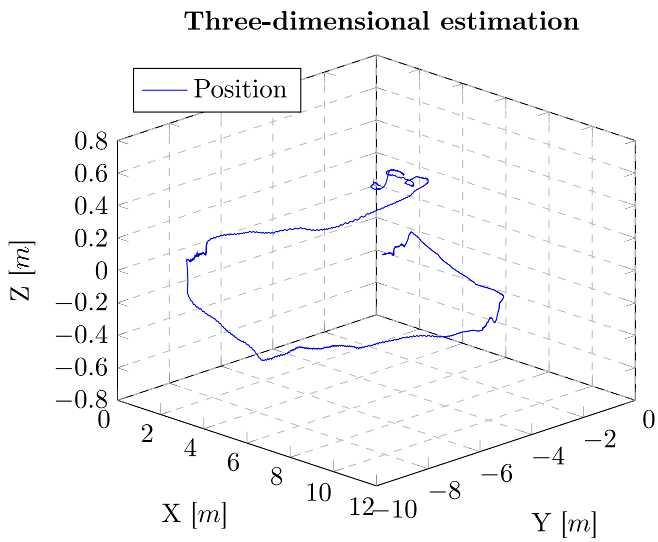

Fig. 14: Same experiment conducted in figure 10 with Z-axis altitude estimation.

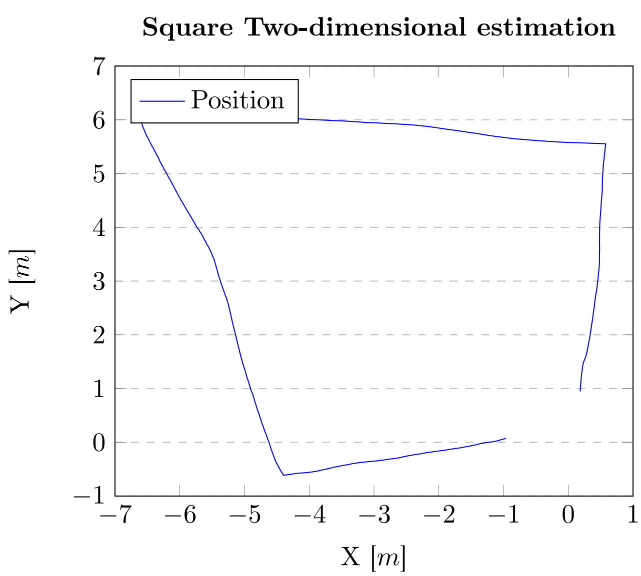

Fig. 15: Same experiment conducted in figure 10 with Z-axis altitude estimation.

reduction normally concedes in accurateness and reliability, although with the recent surge of inexpensive, widely accessible, and precise

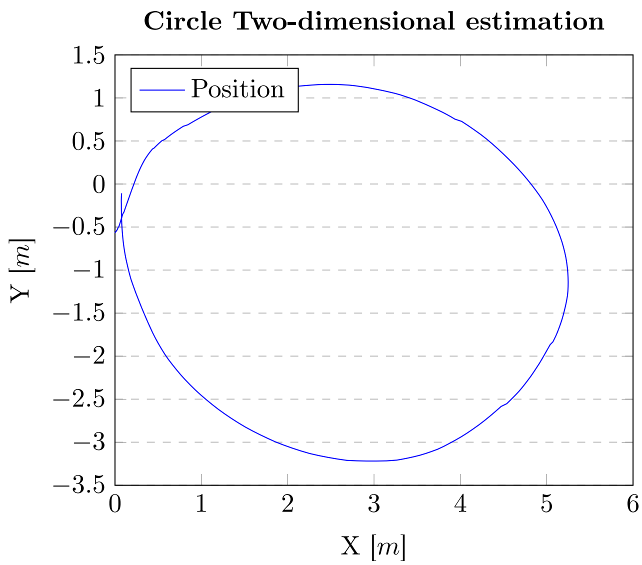

Fig. 16: Same experiment conducted in figure 10 with Z-axis altitude estimation.

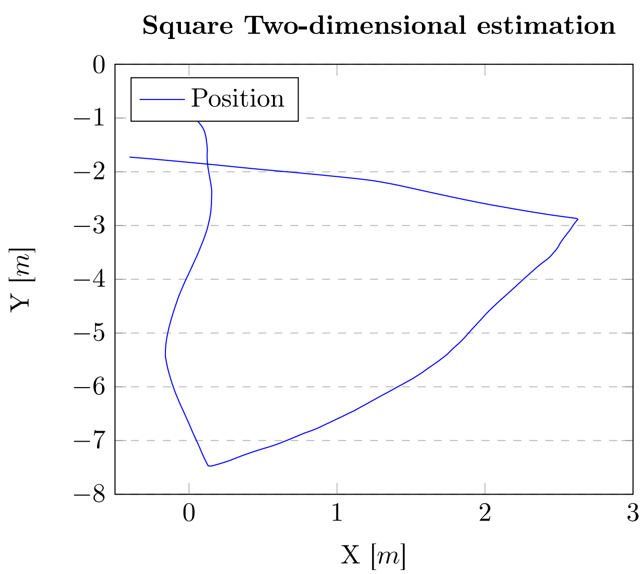

Fig. 17: Same experiment conducted in figure 10 with Z-axis altitude estimation.

microelectromechanical systems (MEMS), that is no longer the case. Still, we aim to employ commercially available tools at the lowest possible cost without compromising the design of a robust and accurate inertial navigation system. A LoPy microcontroller was selected as the navigational computing device of the inertial system, meeting the envisioned requirements for low power with flexible and diverse computational capabilities. The LoPy development board interfaces with the external physical inertial sensor through connection pins (figure 18.a) and communicates remotely by LoRa protocol. A PySense expansion board connects with the LoPy module providing a programable interface for the microcontroller. The inertial navigation system encompasses a small MPU-9250 (figure 18.b) IMU (3x3x1mm) with nine degrees of freedom comprising three accelerometers, three orthogonal gyros, three magnetometers as well as temperature and pressure sensors. This chip is extensively employed in wearable sensors for health, fitness, and sports, motion-based game controllers, and portable gaming. A correct calibration of such sensors is essential for the compensation of their systematic errors, bias, and scale factor. Each time prior to an experiment, the inertial sensor is calibrated while the system is stationary and stabilized to compensate for static error that might corrupt the measurements.

The microcontroller operates MicroPython, a barebones and efficient implementation of Python 3, which incorporates a small subset of the Python standard library. It is optimized to run on microcontrollers and in constrained environments. The inertial module's raw measurements are interpreted by the microcontroller through Inter-Integrated Circuit (I2C) MicroPython driver serial allowing to read the peripherals memory addresses synchronously. The readings of each sensor are later averaged and linearized to better detect and reduce the presence of outlier readings. A fusion algorithm takes as input the averaged data of the accelerometer, gyroscope, and magnetometer. It returns the estimated inertial angles (pitch, roll, and yaw) as well as the projected linear acceleration with a gravity compensation numerical method that utterly removes the effect of the gravity component. Numerically integrating the resultant linear acceleration yields velocity, and double integrating will deliver the body's accumulative position. Merging the AHRS with an accumulative position allows tracking a moving body in three dimensions over time. Moreover, the navigation system is equipped with a LoRa antenna enabling the system to transmit at 868MHz/915MHz LoRa bands in real-time at a long distance the position and orientation information to an external gateway (figure 19). A visualization of the entire hardware solution is provided at image 20.

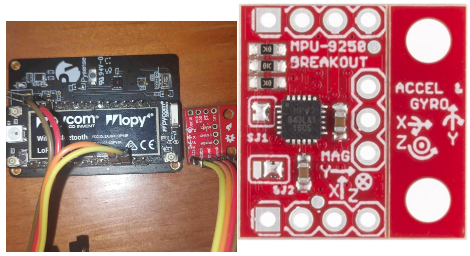

(a) INS Hardware (b) MPU-9250 Breakout

Fig. 18: Pin connection between the microcontroller (left) and the IMU (right). Modules are linked through SCL, CLK, VDD and GND pins.

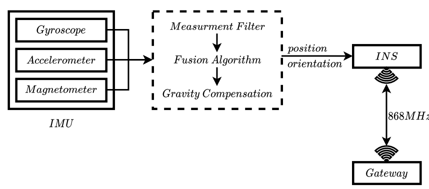

Fig. 19: System overview - Raw measurements from IMU are fused together and numerically integrated to obtain position and orientation. This INS data is transmitted in real-time to a remote node gateway.

4 Results

5 Discussion

TBD

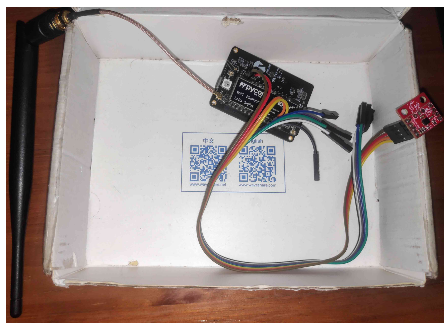

Fig. 20: Complete hardware solution - Box containing the full inertial navigation system, at the left the antenna suitable for use in the 868MHz/915MHz LoRa bands.

References

[1] Moeness G Amin, Pau Closas, Ali Broumandan, and John L Volakis. Vulnerabilities, threats, and authentication in satellite-based navigation systems [scanning the issue]. *Proceedings of the IEEE*, 104(6):1169–1173, 2016.

[2] Jeff Bird and Dale Arden. Indoor navigation with foot-mounted strapdown inertial navigation and magnetic sensors [emerging opportunities for localization and tracking]. *IEEE Wireless Communications*, 18(2):28–35, 2011.

[3] Adam W Bojanczyk and Adam Lutoborski. Computation of the euler angles of a symmetric 3*3 matrix. *SIAM Journal on Matrix Analysis and Applications*, 12(1):41–48, 1991.

[4] Jussi Collin, G Lachapelle, and Jani Käppi. Mems-imu for personal positioning in a vehicle–a gyro-free approach. In *Proceedings of ION GPS*, pages 24–27, 2002.

[5] James L Coyte, David Stirling, Montserrat Ros, Haiping Du, and Andrew Gray. Displacement profile estimation using low cost inertial motion sensors with applications to sporting and rehabilitation exercises. In *2013 IEEE/ASME International Conference on Advanced Intelligent Mechatronics*, pages 1290–1295. IEEE, 2013.

[6] Oliver P Dewhirst, Hannah K Evans, Kyle Roskilly, Richard J Harvey, Tatjana Y Hubel, and Alan M Wilson. Improving the accuracy of estimates of animal path and travel distance using gps drift-corrected dead reckoning. *Ecology and evolution*, 6(17):6210–6222, 2016.

[7] Estefania Munoz Diaz, Fabian de Ponte Müller, Antonio R Jiménez, and Francisco Zampella. Evaluation of ahrs algorithms for inertial personal localization in industrial environments. In *2015 IEEE International Conference on Industrial Technology (ICIT)*, pages 3412–3417. IEEE, 2015.

[8] Wilfried Elmenreich. An introduction to sensor fusion. *Vienna University of Technology, Austria*, 502:1–28, 2002.

[9] Mark Euston, Paul Coote, Robert Mahony, Jonghyuk Kim, and Tarek Hamel. A complementary filter for attitude estimation of a fixed-wing uav. In *2008 IEEE/RSJ international conference on intelligent robots and systems*, pages 340–345. IEEE, 2008.

[10] David L Hall and James Llinas. An introduction to multisensor data fusion. *Proceedings of the IEEE*, 85(1):6–23, 1997.

[11] Evan G Hemingway and Oliver M O'Reilly. Perspectives on euler angle singularities, gimbal lock, and the orthogonality of applied forces and applied moments. *Multibody System Dynamics*, 44(1):31–56, 2018.

[12] Dániel Hetényi, Márton Gótzy, and László Blázovics. Sensor fusion with enhanced kalman filter for altitude control of quadrotors. In *2016 IEEE 11th International Symposium on Applied Computational Intelligence and Informatics (SACI)*, pages 413–418. IEEE, 2016.

[13] Walter T Higgins. A comparison of complementary and kalman filtering. *IEEE Transactions on Aerospace and Electronic Systems*, (3):321–325, 1975.

[14] Rigas Themistoklis Ioannides, Thomas Pany, and Glen Gibbons. Known vulnerabilities of global navigation satellite systems, status, and potential mitigation techniques. *Proceedings of the IEEE*, 104(6):1174–1194, 2016.

[15] Hassan Jameian, Behrouz Safarinejadian, and Mokhtar Shasadeghi. A robust and fast self-alignment method for strapdown inertial navigation system in rough sea conditions. *Ocean Engineering*, 187:106196, 2019.

[16] Aleš Janota, Vojtech Šimák, Dušan Nemec, and Jozef Hrbček. Improving the precision and speed of euler angles computation from low-cost rotation sensor data. *Sensors*, 15(3):7016–7039, 2015.

[17] Wei-Wen Kao. Integration of gps and dead-reckoning navigation systems. In *Vehicle Navigation and Information Systems Conference, 1991*, volume 2, pages 635–643. IEEE, 1991.

[18] Jeong Won Kim, Han Jin Jang, Dong-Hwan Hwang, and Chansik Park. A step, stride and heading determination for the pedestrian navigation system. *Journal of Global Positioning Systems*, 3(1-2):273–279, 2004.

[19] Edward J Krakiwsky, Clyde B Harris, and Richard VC Wong. A kalman filter for integrating dead reckoning, map matching and gps positioning. In *IEEE PLANS'88., Position Location and Navigation Symposium, Record.'Navigation into the 21st Century'.*, pages 39–46. IEEE, 1988.

[20] Quentin Ladetto and Bertrand Merminod. In step with ins navigation for the blind, tracking emergency crews. *Gps World*, 13(ARTICLE):30–38, 2002.

[21] A Tawalbeh Lo'ai, Anas Basalamah, Rashid Mehmood, and Hala Tawalbeh. Greener and smarter phones for future cities: Characterizing the impact of gps signal strength on power consumption. *IEEE Access*, 4:858–868, 2016.

[22] Simone A Ludwig and Kaleb D Burnham. Comparison of euler estimate using extended kalman filter, madgwick and mahony on quadcopter flight data. In *2018 International Conference on Unmanned Aircraft Systems (ICUAS)*, pages 1236–1241. IEEE, 2018.

[23] Simone A Ludwig, Kaleb D Burnham, Antonio R Jiménez, and Pierre A Touma. Comparison of attitude and heading reference systems using foot mounted mimu sensor data: basic, madgwick, and mahony. In *Sensors and Smart Structures Technologies for Civil, Mechanical, and Aerospace Systems 2018*, volume 10598, page 105982L. International Society for Optics and Photonics, 2018.

[24] Chunbo Luo, Sally I McClean, Gerard Parr, Luke Teacy, and Renzo De Nardi. Uav position estimation and collision avoidance using the extended kalman filter. *IEEE Transactions on Vehicular Technology*, 62(6):2749–2762, 2013.

[25] Sebastian Madgwick. An efficient orientation filter for inertial and inertial/magnetic sensor arrays. *Report x-io and University of Bristol (UK)*, 25:113–118, 2010.

[26] Sebastian OH Madgwick, Samuel Wilson, Ruth Turk, Jane Burridge, Christos Kapatos, and Ravi Vaidyanathan. An extended complementary filter for full-body marg orientation estimation. *IEEE/ASME Transactions on Mechatronics*, 25(4):2054–2064, 2020.

[27] AH Mohamed and KP Schwarz. Adaptive kalman filtering for ins/gps. *Journal of geodesy*, 73(4):193–203, 1999.

[28] Mohsen Mosallaei, Karim Salahshoor, and Mohammad Reza Bayat. Process fault detection and diagnosis by synchronous and asynchronous decentralized kalman filtering using state-vector fusion technique. In *2007 3rd International Conference on Intelligent Sensors, Sensor Networks and Information*, pages 209–214. IEEE, 2007.

[29] S Nassar, A Noureldin, and N El-Sheimy. Improving positioning accuracy during kinematic dgps outage periods using sins/dgps integration and sins data de-noising. *Survey Review*, 37(292):426–438, 2004.

[30] Jonathan R Nistler and Majura F Selekwa. Gravity compensation in accelerometer measurements for robot navigation on inclined surfaces. *Procedia Computer Science*, 6:413–418, 2011.

[31] A Noordin, MAM Basri, and Z Mohamed. Sensor fusion algorithm by complementary filter for attitude estimation of quadrotor with low-cost imu. *Telkomnika*, 16(2):868–875, 2018.

[32] Halima Mansour Omar, Zhang Yanzhong, Zhang Bo, and Haris Ubaid Gul. Integration of gps and dead reckoning navigation system using moving horizon estimation. In *2016 IEEE Information Technology, Networking, Electronic and Automation Control Conference*, pages 553–556. IEEE, 2016.

[33] Panagiotis Papadimitratos and Aleksandar Jovanovic. Protection and fundamental vulnerability of gnss. In *2008 IEEE International Workshop on Satellite and Space Communications*, pages 167–171. IEEE, 2008.

[34] Aron Pinker and Charles Smith. Vulnerability of the gps signal to jamming. *GPS Solutions*, 3(2):19–27, 1999.

[35] Honghui Qi and John B Moore. Direct kalman filtering approach for gps/ins integration. *IEEE Transactions on Aerospace and Electronic Systems*, 38(2):687–693, 2002.

[36] K Rahul Sharma, Daniel Honc, and František Dušek. Sensor fusion for prediction of orientation and position from obstacle using multiple ir sensors an approach based on kalman filter. In *2014 International Conference on Applied Electronics*, pages 263–266. IEEE, 2014.

[37] Ulrich Steinhoff and Bernt Schiele. Dead reckoning from the pocket-an experimental study. In *2010 IEEE international conference on pervasive computing and communications (PerCom)*, pages 162–170. IEEE, 2010.

[38] Ross Stirling, Jussi Collin, Ken Fyfe, and Gérard Lachapelle. An innovative shoe-mounted pedestrian navigation system. In *proceedings of European navigation conference GNSS*, volume 110, 2003.

[39] YK Thong, MS Woolfson, JA Crowe, BR Hayes-Gill, and DA Jones. Numerical double integration of acceleration measurements in noise. *Measurement*, 36(1):73–92, 2004.

[40] Harvey Weinberg. Using the adxl202 in pedometer and personal navigation applications. *Analog Devices AN-602 application note*, 2(2):1–6, 2002.

[41] Greg Welch, Gary Bishop, et al. An introduction to the kalman filter, 1995.

[42] Samuel Wilson, Henry Eberle, Yoshikatsu Hayashi, Sebastian OH Madgwick, Alison McGregor, Xingjian Jing, and Ravi Vaidyanathan. Formulation of a new gradient descent marg orientation algorithm: Case study on robot teleoperation. *Mechanical Systems and Signal Processing*, 130:183–200, 2019.

[43] RVC Wong, KP Schwarz, and ME Cannon. High-accuracy kinematic positioning by gps-ins. *Navigation*, 35(2):275–287, 1988.

[44] J Yang, JB Li, and G Lin. A simple approach to integration of acceleration data for dynamic soil–structure interaction analysis. *Soil dynamics and earthquake engineering*, 26(8):725–734, 2006.

[45] Julian Zeitlhöfler. Nominal and observation-based attitude realization for precise orbit determination of the jason sateilltes. 2019.